The Meteoritical Society

Meteoritics & Planetary Science 1–21 (2011)
doi: 10.1111/j.1945-5100.2011.01312.x

Geology and impact features of Vargeão Dome, southern Brazil

Alvaro P. CRÓSTA[1*], César KAZZUO-VIEIRA[2], Lidia PITARELLO[3], Christian KOEBERL[3,4], and Thomas KENKMANN[5]

[1]Institute of Geosciences, University of Campinas, Campinas, Brazil
[2]Petróleo Brasileiro S.A.—Petrobras, Brazil
[3]Department of Lithospheric Research, University of Vienna, Althanstrasse 14, A-1090 Vienna, Austria
[4]Natural History Museum, Burgring 7, A-1010 Vienna, Austria
[5]Institut für Geowissenschaften—Geologie, Albert-Ludwigs-Universität Freiburg, Albertstrasse 23-b, 79104 Freiburg, Germany
[*]Corresponding author. E-mail: alvaro@ige.unicamp.br

(Received 14 December 2010; revision accepted 2 November 2011)

Abstract–Vargeão Dome (southern Brazil) is a circular feature formed in lava flows of the Lower Cretaceous Serra Geral Formation and in sandstones of the Paraná Basin. Even though its impact origin was already proposed in the 1980s, little information about its geological and impact features is available in the literature. The structure has a rim-rim diameter of approximately 12 km and comprises several ring-like concentric features with multiple concentric lineaments. The presence of a central uplift is suggested by the occurrence of deformed sandstone strata of the Botucatu and Pirambóia formations. We present the morphological/structural characteristics of Vargeão Dome, characterize the different rock types that occur in its interior, mainly brecciated volcanic rocks (BVR) of the Serra Geral Formation, and discuss the deformation and shock features in the volcanic rocks and in sandstones. These features comprise shatter cones in sandstone and basalt, as well as planar microstructures in quartz. A geochemical comparison of the target rock equivalents from outside the structure with the shocked rocks from its interior shows that both the BVRs and the brecciated sandstone have a composition largely similar to that of the corresponding unshocked lithologies. No traces of meteoritic material have been found so far. The results confirm the impact origin of Vargeão Dome, making it one of the largest among the rare impact craters in basaltic targets known on Earth.

INTRODUCTION

In Brazil, which covers an area of 8.5 million of km^2, five meteoritic impact structures have been confirmed to date: Araguainha Dome (40 km diameter), Vargeão Dome (12.4 km), Vista Alegre (9.5 km), Serra da Cangalha (13.7 km), and Riachão (4.5 km), plus a possible impact crater, Cerro do Jarau (13.5 km) (Fig. 1a) (Crósta 1982, 1987, 2004; Crósta et al. 2010a). Araguainha, Vargeão, Vista Alegre, and Cerro do Jarau are located in the Paraná Basin, which extends over the central and southern regions of Brazil. Except for Araguainha, which was formed in sedimentary (Permian to Devonian) and crystalline (Neo-Proterozoic) rocks, the remaining three craters of the Paraná Basin were formed in the same stratigraphic unit, the Cretaceous Serra Geral Formation, comprising an extensive flood basalt province. Serra da Cangalha and Riachão were formed in Carboniferous to Permian sedimentary sequences of the Parnaíba Basin, in northern Brazil.

Vargeão Dome, centered at 26°49′S and 52°10′W, is located in Santa Catarina state, and was named after the town located just inside the southern rim of the structure (Figs. 1 and 6). Interstate highway BR-282 cuts across the western portion of Santa Catarina state, providing easy access to the town and to the interior of the structure.

Vargeão, as well as Vista Alegre and the possible Cerro do Jarau structure, were formed in Cretaceous volcanic rocks of the Serra Geral Formation (Crósta et al. 2010a, 2010b). This unit comprises mainly continental flood basalts and subsidiary intermediate and acidic volcanic rocks whose emplacement is related to

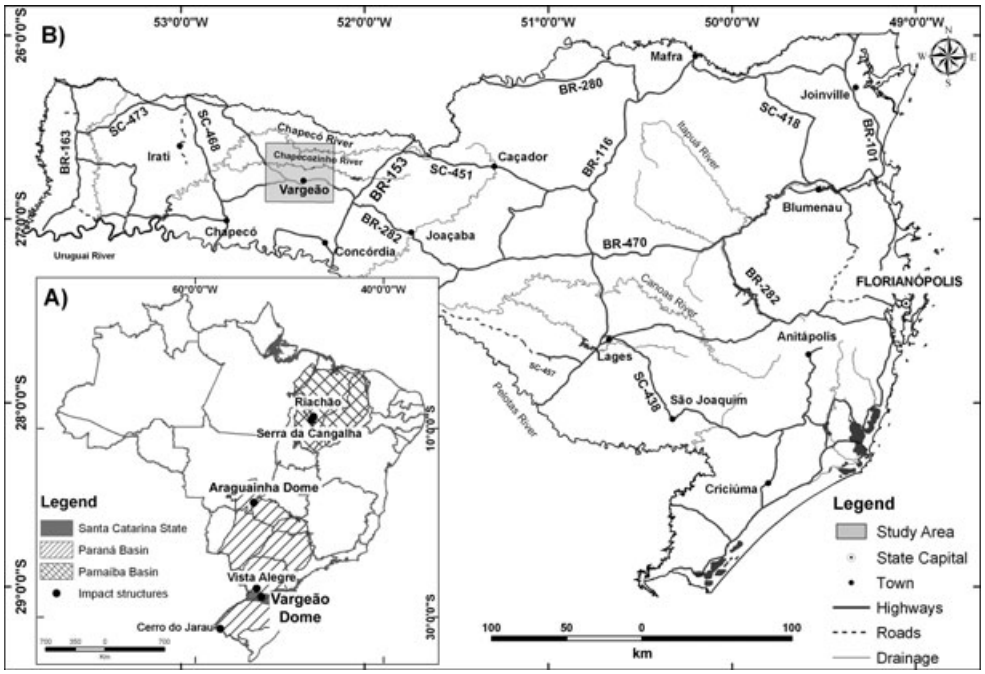

Fig. 1. a) Map of Brazil showing the location of confirmed impact structures in the Paraná and Parnaíba intracratonic basins. b) Map of Santa Catarina State, with the location of the town of Vargeão.

the rifting of Gondwana and the formation of the South Atlantic Ocean (Peate et al. 1992; Renne et al. 1992; Peate and Hawkesworth 1996; Milani 2004).

Although common on other planetary surfaces, impact craters in basalt are rare on Earth. Among the few known craters formed in basaltic rock are Lonar crater in India and Logancha in Eastern Siberia, Russia. Lonar is a simple and well-preserved crater formed in the basalts of the Deccan Traps ≤0.05 Ma ago (e.g., Fredriksson et al. 1973; Fudali et al. 1980; Sengupta and Bhandari 1988; Osae et al. 2005; Maloof et al. 2010). Logancha is a complex crater formed on the Tunguska basin, excavated from a 1 km-thick Triassic basalt plateau and Permian sediments (Feldman et al. 1983; Mironov et al. 1987). However, the information on Logancha available in the international literature is very limited and the severely eroded structure exposes only Permian sediments (cf. Son and Koeberl 2007).

Thus, Lonar, together with Vargeão Dome, Vista Alegre, and possibly Cerro do Jarau, are the few meteorite craters known on Earth so far which may provide ground information on impact effects in basalt targets.

Here, we present a summary of the geology of Vargeão Dome, comprising morphologic and structural characterization, description of the rock types that occur in the interior of the structure, as well as new data on shock features and new petrographic descriptions of recently collected shocked lithologies. Besides presenting new data, a major goal of the present study was to provide a summary of the geology and impact features of Vargeão Dome, as very little information about this impact structure has so far been available in the international literature.

PREVIOUS WORK

The first reference to the existence of a large circular structure in Vargeão was by Paiva Filho et al. (1978). These authors described Vargeão Dome as a circular depression imprinted in igneous rocks of the Serra Geral Formation, with outcrops of sandstones near its center. The sandstones were correlated by these authors to the Triassic-Jurassic Pirambóia/Botucatu formations, and they pointed out that the topographic position of these rocks was at least several hundred meters above their normal level of occurrence in this part of the Paraná Basin. As for the possible origin for this structure, they suggested a cryptomagmatic intrusion of alkaline nature, similar to other Cretaceous intrusions that occur in the western portion of Santa Catarina State near the towns of Lajes and Anitápolis.

During the 1980s, oil/gas exploration surveys were conducted in this portion of the Paraná Basin, and Vargeão Dome was targeted as a potential hydrocarbon trapping structure. In a report of one of these surveys Barbour and Corrêa (1981) observed that the sandstone outcrops at the center of the structure were structurally

controlled, bounded by faults along the contacts with the volcanic rocks of the Serra Geral Formation. The authors reported on the occurrence of breccias in the interior of the structure that they considered to be of tectonic origin and related the brecciation to the same event responsible for the uplift of the sandstones. They presented a list of geologic processes that might have formed Vargeão Dome: faulting (with vertical displacements of up to 500 m), volcanic explosion with the formation of a caldera, alkaline igneous intrusion, and meteorite impact. As part of this oil/gas survey, reflection seismic data were also acquired in a section across the structure.

A possible impact origin of Vargeão Dome was first proposed by Crósta (1982), based on morphologic and tectonic similarities between Vargeão Dome and other eroded impact craters, including Araguainha Dome. Crósta (1987) mentioned the occurrence of possible monomict impact breccias formed in basalt of the Serra Geral Formation and planar microstructures in quartz grains from the sandstone outcrops at the center of Vargeão, which pointed toward an impact origin of Vargeão Dome.

Hachiro et al. (1993), in a conference article, referred to possible evidence of shock found in sandstone and volcanic rocks from the interior of Vargeão Dome. They claimed to have found PDF (planar deformation features) in quartz and feldspar crystals, as well as diaplectic glass within sandstones, whereas in volcanic rocks of the Serra Geral Formation, they described deformation features, such as fracturing, rotation, and grinding of feldspar crystals; however, no pictures or data in support of these claims were presented.

Crósta et al. (2006) presented a summary of the geology and impact evidence of Vargeão Dome, comprising shatter cones in sandstone of the Botucatu/Pirambóia formations, different types of monomict impact breccias formed in basalts and sandstones, and planar features in quartz.

Kazzuo-Vieira et al. (2009) used geophysical data (airborne magnetics and reflection seismic data) to identify a relatively shallow crustal structure with a strongly deformed zone underneath. The seismic interpretation shows the presence of a central uplift, elevating sandstones of the Botucatu/Pirambóia formations from a depth of approximately 1000 m to the surface.

METHODS

Remote Sensing Data

The morphologic and structural characterization of Vargeão Dome was carried out using satellite optical and microwave remote sensing data. ASTER (Advanced Spaceborne Thermal Emission and Reflection Radiometer) is a 14-band multispectral sensor operating onboard NASA's Terra satellite, with spatial resolutions ranging from 15 m in the visible and near-infrared ranges of the electromagnetic spectrum (3 bands), 30 m in the shortwave infrared (6 bands), and 90 m in the thermal infrared (5 bands) (Abrams 2000). ASTER is a geologically oriented sensor, and the combination of spatial and spectral information provided by this sensor has been useful for mapping structures and lithologies related to Vargeão Dome. RADARSAT-1 is a C-band (5.3 gigahertz) spaceborne radar with configurable imaging modes operated by the Canadian Space Agency (Brown et al. 1996), and the scene used for analyzing Vargeão Dome was acquired in Standard 7 mode, with a spatial resolution of 12.5 m. Shuttle Radar Topography Mission (SRTM) digital elevation data were acquired by a C-band dual-antenna interferometric radar system operating onboard NASA's Endeavour Space Shuttle (Rabus et al. 2003). The SRTM data available have a spatial resolution of 3-arc-second (equivalent to approximately 90 m per pixel).

The multispectral ASTER data were processed for enhancing both textural and spectral contents, allowing the extraction of structural and lithologic information, respectively. SRTM data were used for regional structural and morphologic analyses, after being processed using shaded relief and pseudocoloring techniques to enhance subtle textural features related to geologic structures of Vargeão Dome. RADARSAT-1 data were improved by applying a noise reduction filter (speckle filtering) and then by a sharpening filter to enhance structural elements.

Processed remote sensing data were subsequently used for recognizing different lithologies and identifying structural features related to the structure and the surrounding area. The results were spatially integrated and analyzed in conjunction with existing geologic maps in a GIS (geographic information system) environment.

Reflection Seismic Data

Seismic data were supplied by ANP (Brazilian National Petroleum and Gas Agency) and were acquired in 1982 by PETROBRAS (Petróleo Brasileiro S/A). Seismic line 0236-0078 cut across the structure along the ENE/WSW direction. It comprises 1264 shots, spaced at 15 m. Each shot has 240 groups of receivers, with spacings of 30 m between receivers, in a split-spread configuration (120 groups of receivers at each side of the shot point). The register time was 4 s with a sample rate of 2 ms, but only 2 s was processed.

Processing of seismic data was carried out using the standard procedure proposed by Yilmaz (2001) with the

objective of enhancing geologic and structural features located underneath the Vargeão structure. In addition, F-K-filtering was used to attenuate the strong S-waves present in the data. A description of the procedure used for processing the Vargeão seismic data is given by Kazzuo-Vieira et al. (2009).

Petrographic and Geochemical Analysis

The samples used in this study were collected during several field campaigns between 2003 and 2010. Petrographic analysis was conducted on selected samples that are representative for the variety of lithologies present. The petrographic characteristics of the samples were studied in Campinas and Vienna by optical and electron microscopy on normal and polished thin sections, respectively. Shock effects in quartz were also studied at the University of Freiburg, Germany, with a Leica polarizing microscope. Electron microscopy was performed at the University of Vienna, Austria, with a FEI-Inspect S50 scanning electron microscope (SEM). In addition, the composition of single phases was determined by wavelength-dispersive microprobe analysis, using a Cameca SX 100 instrument equipped with four wavelength-dispersive spectrometers and an energy-dispersive spectrometry system. Data reduction was performed using standard ZAF procedures.

A suite of seven representative samples was selected for chemical analysis. The selection criteria were: fresh appearance, distribution, and abundance in the structure and possibility of comparison with the data in literature. From the Serra Geral Formation, we selected two representative endmembers, basalt and rhyodacite. Representative aliquots weighing about 20–30 g of the selected samples were crushed in polyethylene wrappers and powdered in a mechanical agate mill for bulk chemical analysis. The contents of major and trace (V, Ni, Cu, Zn, Rb, Sr, Y, Zr, Nb, Ba, and Pb) elements were determined by X-ray fluorescence (XRF) spectrometry, using a Philips PW2400 instrument. Abundances of some major and trace elements were determined by instrumental neutron activation analysis (INAA). The obtained results were then integrated and compared with the XRF data. All analyses were conducted at the Department of Lithospheric Research, University of Vienna, Austria. Details of the methods (quantities, instrumentation, standards, accuracy, precision, etc.) are in, for example, Koeberl (1993) and Mader and Koeberl (2009).

GEOLOGIC SETTING OF VARGEÃO DOME

Vargeão is located within the extensive igneous province of southern Brazil, in the central portion of the Paraná Basin (Fig. 2). To help understand the setting of

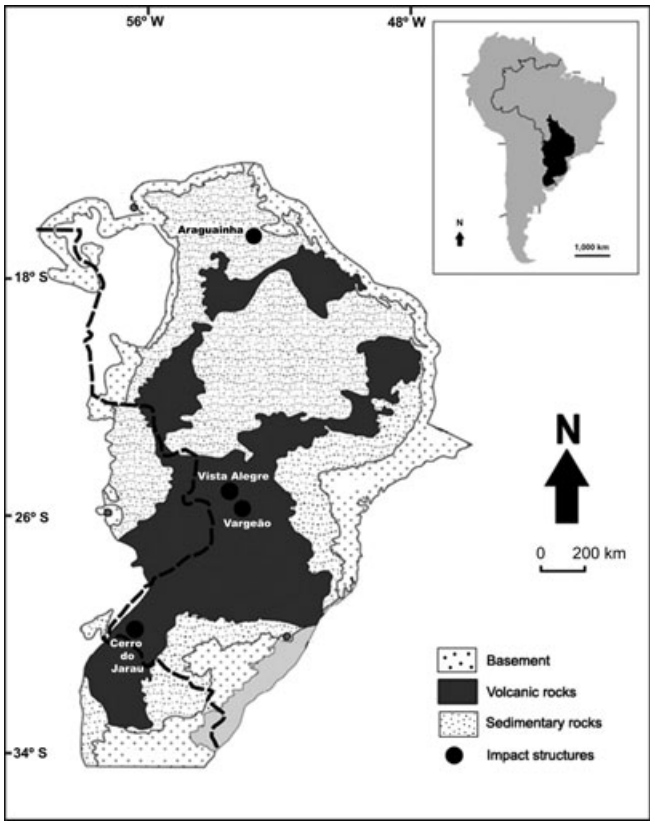

Fig. 2. The Paraná Basin and its main volcano sedimentary sequences. The volcanic sequence is represented by continental flood basalt and related intermediate to acidic volcanic rocks of the Serra Geral Formation. The four impact structures of the Paraná Basin are indicated.

Vargeão and its target rocks, we provide herein a brief summary of the regional geology. This basin contains undeformed sedimentary volcanic sequences deposited between the Silurian and Cretaceous, and covers a total area of about 1.5 million km^2 in central-southern Brazil, as well as in Uruguay, Paraguay, and Argentina.

The breakup of Gondwana around the Jurassic-Cretaceous transition between 137.8 ± 0.7 and 126.8 ± 2.0 Ma, resulted in extensive continental volcanism in the Paraná Basin (Stewart et al. 1996; Peate 1997), represented by the Serra Geral Formation. The igneous activity comprises widespread lava flows and intrusions. Lava flows covered approximately 75% of the surface of the entire basin, and the maximum thickness of the volcanic sequences reached up to 2 km. In terms of composition, 90% by volume are rocks of basic composition, whereas the other 10% are rocks of intermediate to acidic compositions (Peate et al. 1992; Peate and Hawkesworth 1996).

The rocks in the region are part of the São Bento Group. It consists, from top to bottom, of the Serra Geral Formation, the Jurassic/Cretaceous Botucatu

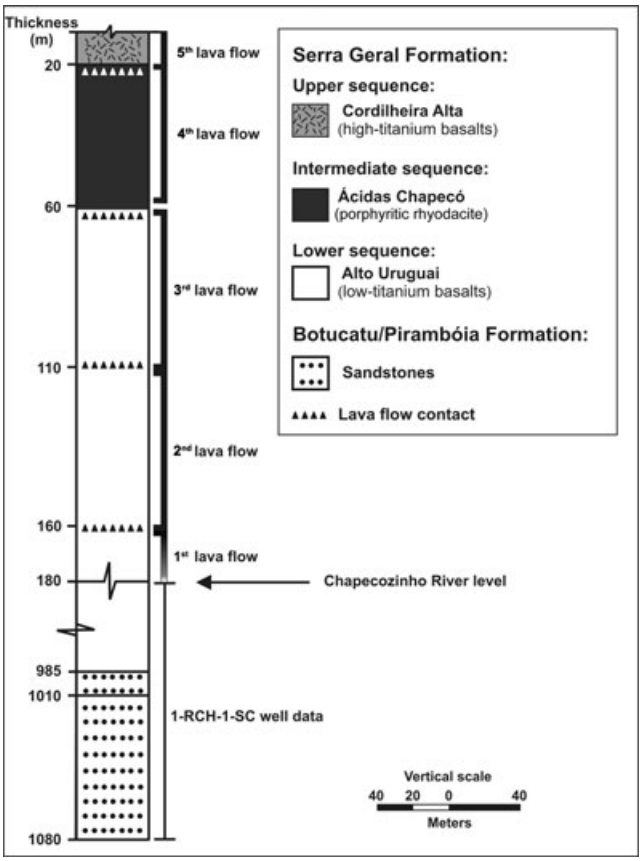

Fig. 3. Stratigraphic column of the Serra Geral Fm. (igneous sequence) and Botucatu/Pirambóia Fm. (sedimentary sequence). The succession of five lava flows and their respective thicknesses are based on field observations at Vargeão Dome and surroundings, whereas the lower part of the column is based on data from the 1-RCH-1-SC oil well (ANP 1981). The upper volcanic sequence (Cordilheira Alta) does not occur at Vargeão.

Formation, and the Triassic/Jurassic Pirambóia Formation. These sedimentary and volcanic units of the São Bento Group comprise the rock types exposed at Vargeão Dome (Fig. 3). Underlying the São Bento Group, there are, from top to bottom, the Passa Dois Group, the Taciba Formation, and the Furnas Formation.

The volcanism that generated the Serra Geral Formation was dated between 139 and 125 Ma by the $^{40}Ar/^{39}Ar$ method (Renne et al. 1992; Turner et al. 1994). Using the same method, Mantovani et al. (1995) suggested the occurrence of two peaks of volcanic activity, one at 138–135 Ma and the other at 133–128 Ma.

In the western portion of Santa Catarina state, where Vargeão Dome is located, the Serra Geral Formation was divided by Freitas et al. (2002) into distinct stratigraphic units: a lower sequence of tholeiitic basalt named Alto Uruguai, two intermediate sequences of acidic volcanic rocks named Palmas and Chapecó, and an upper sequence of tholeiitic basalt called Cordilheira Alta (Fig. 3).

The clastic and volcanic rocks of the São Bento Group, as well as most of the rocks of the Paraná basin, have not been affected by any major postdepositional tectonic deformation event.

MORPHOLOGIC AND STRUCTURAL ASPECTS

The regional geomorphology of the western region of Santa Catarina state is characterized by a highly dissected terrain, related to the areas of the basaltic lava flows, where river valleys (e.g., the Irani and Pelotas rivers) are deeply incised into the surface. This dissection of the basalt is favored by chemical weathering of these iron-rich rocks under the prevailing subtropical conditions.

In contrast, the areas where the acidic volcanic flows occur are considerably more resistant to chemical and physical weathering. Consequently, these areas exhibit dissimilar morphological patterns, with more flat plateaus combined with narrow and deep river valleys (e.g., the Chapecó and Chapecozinho rivers).

In this geomorphologic context, and occurring near the limit between these two different terrains, Vargeão Dome stands out as a remarkable circular anomaly (Fig. 4). The structure exhibits a sharp and steep border, with topographic gradients reaching more than 200 m, as well as an internal concentric multiannular pattern and a slightly elevated central portion. These aspects are illustrated in Fig. 4, which shows a close-up of the SRTM digital elevation model.

The morphology of the structure was further investigated using synthetic aperture radar (SAR) data from the Radarsat-1 sensor, which is very sensitive to surface roughness, and therefore, is useful for enhancing morphologic features. Figure 5a shows the Radarsat-1 image, in which the concentric and radial lineaments associated with the Vargeão Dome structure were traced, as well as the rim of the structure. A closer view of this region near the rim of the structure is presented in Fig. 5b, as seen by the ASTER sensor, with a spatial resolution of 15 m. Again, multiple parallel concentric lineaments are prominent, although not exposed continuously mostly due to agricultural use. These lineaments are interpreted herein as the surface expression of the normal (or listric) faulting that was responsible for the formation of the outer rim of the structure.

GEOLOGY OF VARGEÃO DOME

Figure 6 shows a schematic geological map of the Vargeão Dome, with the lithologic types identified in the interior of the structure.

In portions of the rim of Vargeão Dome that are somewhat protected from erosion, such as in the southern section, four different lava flows can be recognized. The

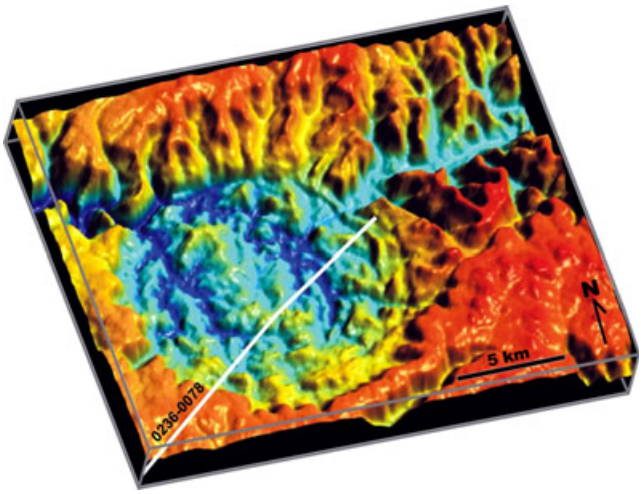

Fig. 4. Three-dimensional perspective view of the regional SRTM digital elevation model of the Vargeão Dome, exhibiting its steep rim, with topographic gradients reaching more than 200 m, as well as an internal concentric multiannular pattern and the slightly elevated central region. Line 0236-0078 shows the location of the segment of the seismic line across Vargeão Dome presented in Fig. 15.

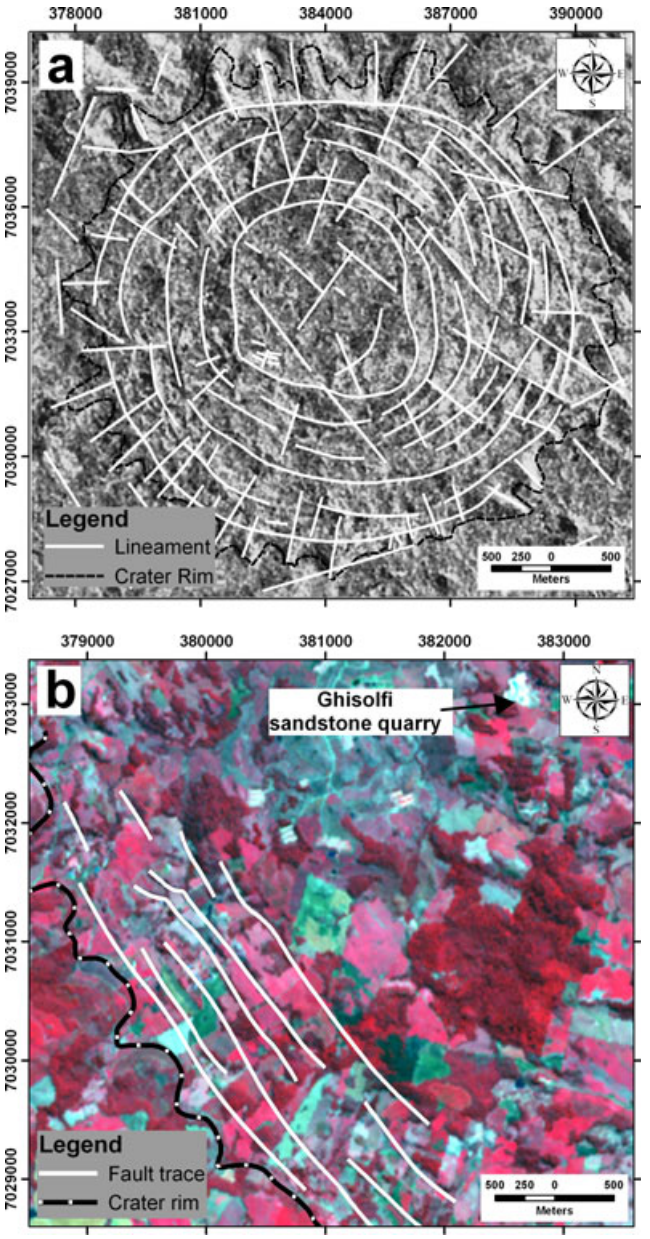

Fig. 5. a) Radarsat-1 image, showing multiple concentric and radial lineaments, interpreted as normal or listric faults. b) ASTER image, showing the interpreted annular and concentric normal or listric faults in the southwestern rim of the Vargeão Dome. Coordinate system is in Universal Tranverse of Mercator (UTM), zone 23 South.

uppermost flow comprises porphyritic rhyodacite of the Ácidas Chapecó unit, whereas the other three are basalt of the Alto Uruguai unit (Fig. 7a). These rocks represent the lithologies in which the Vargeão Dome was formed, and from the BR-282 highway toward the town of Vargeão, they can be observed almost fresh and completely undeformed in road cuts along the 3 km-long access to Vargeão, locally exhibiting characteristics that allow the separation between distinct lava flows (Fig. 7b). Figure 7c shows the characteristics of the porphyritic rhyodacite with plagioclase phenocrysts typical of the Ácidas Chapecó unit. The topographic gradient between the external plateau outside the rim and the lower part of the town of Vargeão is approximately 180 m, indicating an average thickness of approximately 45 m for individual lava flows. In addition, in several places around the rim, in the inner part of the structure, large blocks (up to several hundred meters long) of undeformed volcanic rocks from the two units (Ácidas Chapecó and Alto Uruguai) can be seen, sometimes tilted, suggesting that they collapsed from the rim into the interior of the structure. The fault planes along which these blocks were displaced in a downward direction have been recognized at several locations around the inner part of the rim (Fig. 7d).

Sandstone occurrences at Vargeão are restricted to the central part of the structure. They occur as blocks of up to several hundred meters in size, arranged in a circular ring around the center of the structure, as shown in Fig. 6. These sandstones have been attributed by Paiva Filho et al. (1978) and Crósta et al. (2006) to the Botucatú and/or Pirambóia formations, which in this portion of the Paraná Basin lie at a depth of approximately 1000 m. This depth is indicated by data from the oil exploration well 1RCH-0001-SC, located 22 km from the rim of Vargeão Dome toward the northeast, and in which the Botucatu Formation was found at 980 m depth and the Pirambóia Formation at 1100 m (ANP 1981). However, it is not possible to

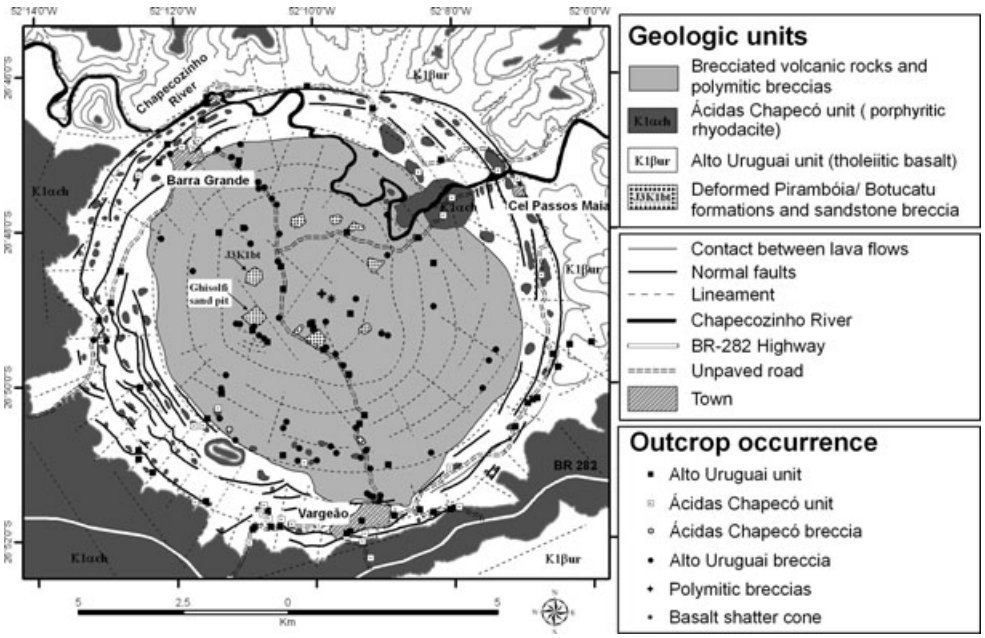

Fig. 6. Schematic geological map of Vargeão Dome.

unambiguously relate these sandstones to either the Pirambóia or Botucatu formations, mainly because they are intensely deformed and recrystallized as a result of the uplift of these rocks (Kazzuo-Vieira 2009).

The types of rocks found in the interior of Vargeão Dome comprise unshocked/slightly to moderately fractured basalt and rhyodacite located in a collar near the rim (Fig. 6), and brecciated/fractured/melted rocks, which include these two volcanic rock types plus the sandstones. The latter group may involve one single rock type as monomict breccias, or more than one at varied proportions as polymict breccias. In the geological map of Fig. 6, with the exception of the sandstones, these breccias have been grouped into a single unit called ''brecciated volcanic rocks'' (BVR), because the lack of continuous exposures and the current level of mapping of these breccias types is not sufficient to separate the distinctive types.

Brecciated Volcanic Rocks

The brecciated volcanic rocks (BVR) at Vargeão Dome contain clasts of dark gray basalt and/or rhyodacite in a poorly sorted and heavily oxidized matrix of intense red color, and they are found in extensive outcrops in several areas in the interior of the structure, such as the one just north of the town of Vargeão (Fig. 8a). The volcanic clasts, in turn, are usually strongly fractured, with the fractures being filled by a red material. These red veinlets comprise finely comminuted fragments in an oxidized matrix, similar to the matrix of the BVRs (Fig. 8b). Clasts of basaltic composition are the most frequent components in these breccias (Fig. 8c), although in some places, as in the central-southern part of the structure, clasts comprise also rhyodacite. The degree of brecciation varies considerably at different places. All the interstices and fractures among the clasts are filled with an intensely oxidized matrix, thus making the more brecciated varieties appear more reddish compared to the less brecciated varieties, which appear light gray. Locally, the BVR contain portions with fluidal texture (dark color) comprising glassy material (Fig. 8d). In one of the freshly cut samples of the BVR, a few flecks of native copper up to a few millimeters in size were observed in fracture fills (Fig. 8e).

Under the optical microscope, the red veinlets appear to have been injected into the basaltic fragments. The veins vary in thickness: (1) veins thicker than about 1 mm show internal layering, with dark red layers containing basalt clasts alternating lighter red layers containing quartz or sandstone clasts (Fig. 9a), (2) veins thinner than 1 mm are injected into the basalt, forming a network without a preferred orientation; clasts in these veins are almost totally absent, except for a few fragments of basalt that are spalled off the margins. Locally, the thicker veins show a gradual transition to the host basalt, with cataclastic bands along the margins of the veins. Such cataclastic layers consist of fine-grained (tens of μm) angular fragments of plagioclase and pyroxene. The thicker veins contain fragments ranging from a few μm to several mm in size. Fragments include shocked and unshocked sandstones that preserve

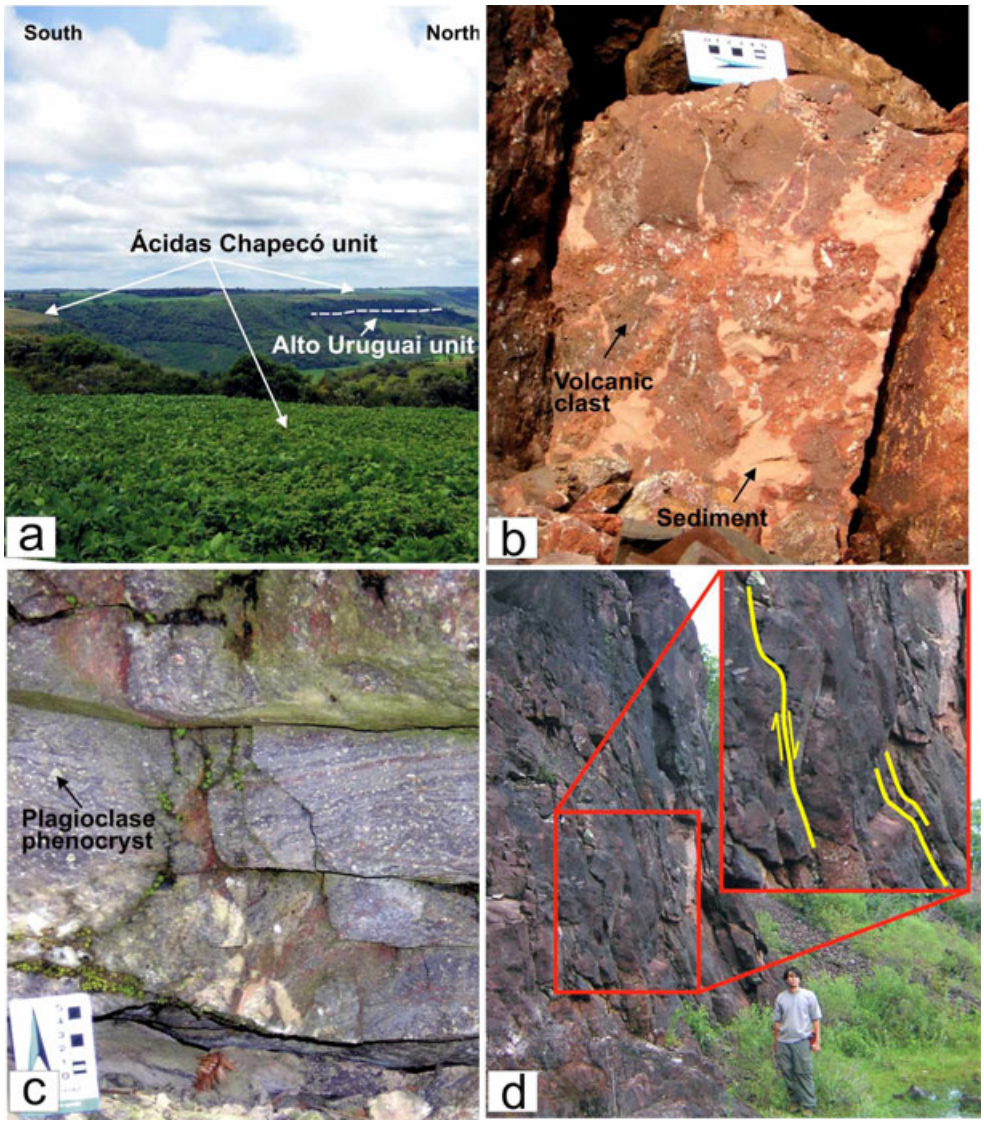

Fig. 7. a) Partial view of the SW rim of Vargeão Dome showing the Ácidas Chapecó unit that forms the plateaus around the structure. b) Upper portion of the Alto Uruguai individual flow, comprising peperitic breccia formed by vesicular basalt fragments mixed with fine-grained sediments (siltstone). c) Outcrop of the Ácidas Chapecó unit along the road descending from the rim toward Vargeão town, comprising porphyritic rhyodacite with flow structure and euhedral plagioclase phenocrysts. d) Normal faults affecting basalt from the Alto Uruguai unit at the SW inner part of the rim, near Vargeão town.

the original layering (Fig. 9b), shocked and unshocked basalts, and minor amounts of other volcanic rocks, fragments of devitrified glass, and single grains of, in order of decreasing abundance, quartz, plagioclase, and calcite. The shape of the fragments in the matrix is generally angular and no evidence of melting along margins was observed, but locally the matrix contains melt portions (Fig. 9c). The basalt clasts, on the contrary, are well rounded and comprise aggregates of pyroxene and plagioclase. The basalt into which this kind of veinlet is injected appears strongly altered, but the composition of the single preserved phase is consistent with that of the original basalt.

The averaged chemical compositions of three samples of BVR are shown in Table 1, compared to the compositions of unshocked basalt, rhyodacite, and Botucatu sandstone. The average bulk composition of BVR reflects the composition of the Serra Geral basalts (Figs. 10a–c), except for a slight enrichment in silica, whereas the trace element data do not show any difference. The BVR composition is similar to that of the basalt, but slightly shifted toward the rhyodacite.

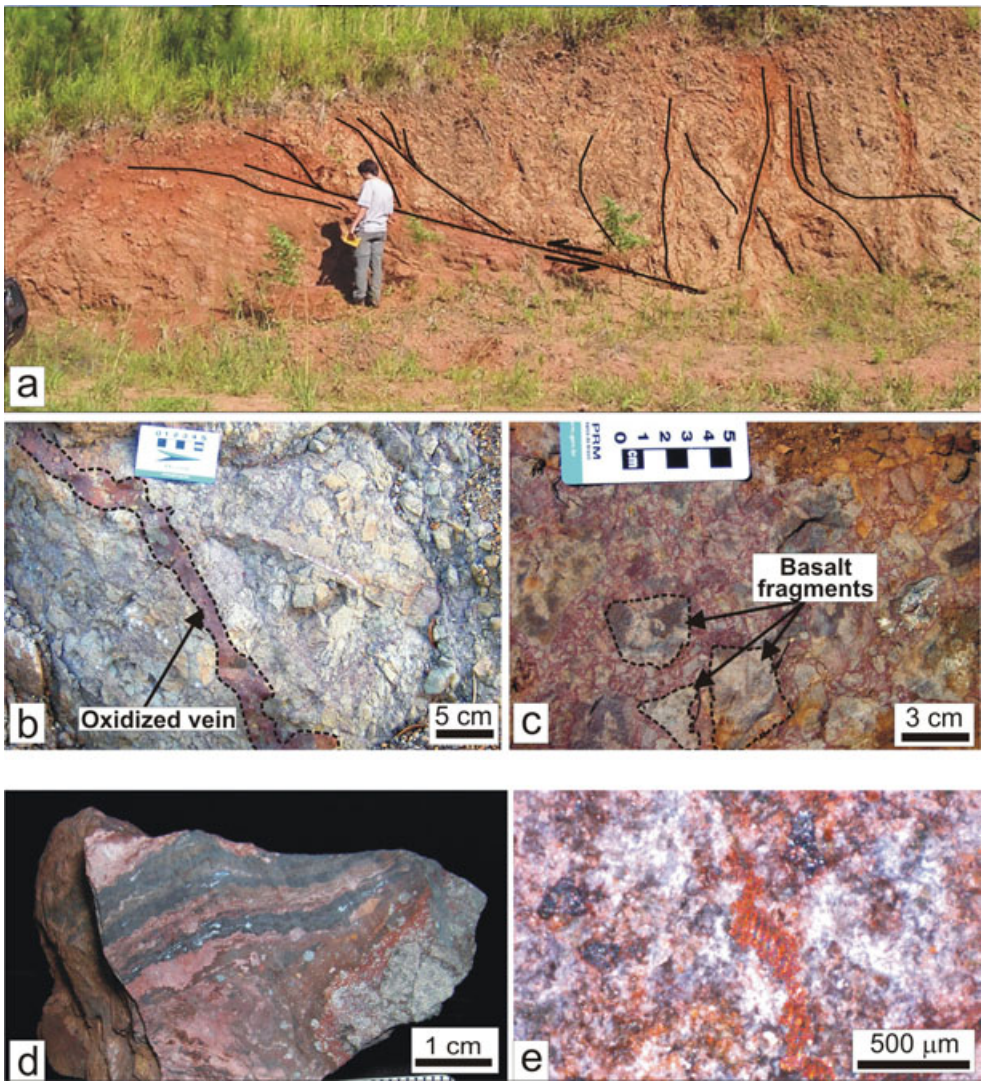

Fig. 8. a) Faulted blocks of brecciated volcanic rocks (BVR) exposed in a road cut 2 km north of the town of Vargeão. b) Clasts of dark gray basalt in poorly sorted and heavily oxidized matrix of intense red color, exhibiting a red fracture fill; the vein comprises finely comminuted fragments in an oxidized matrix, similar to the matrix of the BVR. c) BVR with cm size, altered basalt fragments embedded in an oxidized matrix. d) BVR exhibiting melt segments with fluidal texture. e) BVR with flecks of native copper filling fracture.

Polymict Breccias

Although some of the BVR may contain minor fragments of sandstone, these could have originated from intertrap sandstones, from the upper portions of a lava flow. Therefore, the term ''polymict breccia'' is employed herein to designate breccias that have distinct contributions from volcanic rocks of the Serra Geral Formation, as well as from sandstones of the Botucatu/Pirambóia formations. These rocks have been found only at two localities within the Vargeão Dome, comprising two nearby meter-sized outcrops located near the center of the structure (see geological map of Fig. 6 for location of these outcrops).

The polymict breccias are generally composed of angular mm-sized basalt clasts and minor amounts of sandstone and calcite clasts set in a fine-grained red matrix (Fig. 11a). The matrix is reddish and is composed of μm-sized comminuted basalt, rhyodacite, quartz, and calcite clasts, as well as some unidentified fine-grained material. At higher magnification, the matrix contains more angular quartz clasts than volcanic minerals. The clasts have two different sizes: (1) mm- to cm-sized fragments of shocked and unshocked basalt and sandstone (Figs. 11b and 11c), (2) single clasts, less than 1 mm in size, of quartz, calcite, feldspar, and rare pyroxene. Some large (mm-sized) fragments of basalt

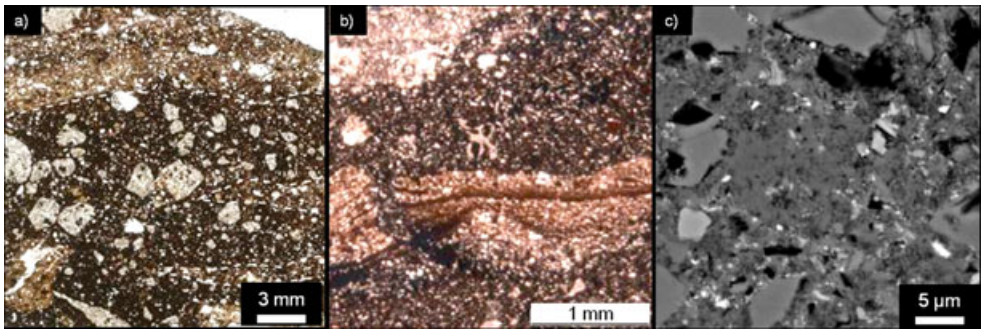

Fig. 9. Microscopic features of the BVR. a) BVR vein with different generations of melt. The contact is marked by a dashed white line. One generation has darker matrix and contains mostly basalt clasts. The other generation has lighter matrix and contains smaller-sized fragments composed mainly of sandstone. Plane-polarized light image. b) Microphoto of a sandstone clast included in the BVR matrix, preserving the original layering, marked by a different grain size and hematite content. Plane-polarized light image. c) Detail of the "matrix" which contains some melted portions (homogeneous gray at the image center) surrounded by angular clasts of plagioclase (dark gray) and pyroxene (light gray). Backscattered electron image.

show intensely fractured pyroxene, partially replaced by iron oxides along fractures, grain boundaries, and cleavage/exsolution planes, and plagioclase transformed into diaplectic glass, completely extinct under cross-polarized light, but preserving the magmatic elongate shape of crystals (Figs. 11c and 11d). Single quartz and feldspar grains generally appear unaltered and devoid of shock features, but locally some quartz grains show intense fracturing and incipient formation of planar fractures and feather features. Some calcite grains show kinked or plastically deformed polysynthetic twins. Melt clasts are rare and consist of dark red fragments showing internal fluidal fabric or containing white rounded small crystals (Fig. 11e).

Monomict Sandstone Breccias

The sandstone breccias occur in the central part of Vargeão Dome as a concentric ring of discontinuous and fault-controlled blocks (Fig. 6). Their contact with the BVR appears to be of tectonic nature, due to faulting related to the formation of the crater, and they commonly occur as very hard, meter-sized blocks of recrystallized sandstone ("quartzites") found at the surface, usually on topographic highs. However, at a few sites, such as the large Ghisolfi sandstone pit, they have been excavated at depths of several tens of meters, exposing vertical profiles in which intense deformation (such as folding and faulting) can be observed. The deformation is conspicuous at all scales, but is spatially heterogeneous; meter-sized blocks appear unaffected by deformation, whereas zones around them are deformed. In most of the preserved blocks, the original bedding is subvertical. Monomict breccias in sandstone are common, and the original bedding is frequently displaced by faulting.

Microscopically, most of the deformed sandstone and sandstone breccias comprise sandstone fragments embedded into an unoxidized matrix composed of submillimeter-sized quartz fragments. Nevertheless, at a single site, an oxidized 3–4 cm-thick vein was observed in a sandstone breccia, comprising undeformed quartz grains mixed with fragmented quartz in an aphanitic oxidized matrix (Fig. 12a).

Undeformed sandstone in the breccia contains well-rounded quartz grains. Quartz grains are mostly monocrystalline, and no deformation and recrystallization were observed within the single grain. The quartz grains are cemented by pure silica and hematite. The silica cement shows textures, such as fringes and mosaic growth, which are typical for diagenetic processes. In the cement, mica sheets are locally entrapped. The sandstones also have minor amounts of well-rounded grains of plagioclase, microcline, and microcrystalline silica (chert).

The sandstone breccia is characterized by centimeter-sized sandstone clasts immersed in a highly fragmented quartzose matrix (Fig. 12b). The sandstone clasts, some of which are slightly deformed, are composed of rounded quartz grains. The deformation, mainly in the matrix, is progressively localized into conjugate sets of shear bands, mm to cm in thickness, and composed of comminuted and recrystallized quartz grains that are 10–100 μm in size (Fig. 12c).

The portions of less deformed sandstone, isolated by the shear bands, show aggregates of rounded quartz grains of 400–500 μm size. In the less deformed portions, some residual porosity is preserved, but the original layering is completely obliterated. Rounded quartz grains show radial fractures that emanate from the contact with the neighboring grains, and contain abundant fluid inclusions trails. Larger grains locally exhibit undulose extinction, deformation bands, and incipient recrystallization, with less deformed cores surrounded by subgrains and recrystallized grains,

Table 1. Major and trace element contents in samples collected outside the studied structures of target rock equivalents compared to shocked lithologies from within the structure.

	Samples collected outside the structure			Shocked lithologies	
	Serra Geral basalt	Rhyodacite	Botucatu sandstone	Brecciated volcanic rocks (average $n = 3$)	Monomict sandstone breccia
SiO_2	51.55	68.85	95.11	54.9 ± 2.8	98.16
TiO_2	1.82	1.32	0.08	2.27 ± 0.05	0.08
Al_2O_3	12.46	11.47	1.27	11.1 ± 1.0	0.33
Fe_2O_3	15.73	6.55	0.27	14.9 ± 0.4	0.20
MnO	0.26	0.12	< 0.01	0.20 ± 0.02	< 0.01
MgO	3.82	0.58	0.11	3.53 ± 1.18	0.08
CaO	7.86	1.80	1.18	6.89 ± 1.18	0.06
Na_2O	2.86	2.62	0.12	2.22 ± 0.22	0.11
K_2O	1.38	3.59	0.50	1.80 ± 0.63	0.06
P_2O_5	0.22	0.36	0.03	0.29 ± 0.08	0.03
LOI	0.69	1.45	0.96	0.89 ± 0.35	0.19
Total	98.65	98.71	99.63	98.97	99.30
Sc	39.1	11.0	0.84	35.9 ± 4.5	0.19
V*	550	28.9	7.9	332 ± 94	4.3
Cr	36.6	4.60	4.57	39.1 ± 22.0	1.39
Co	44.0	5.95	0.77	33.2 ± 5.9	0.16
Ni*	31.9	0.9	1.7	25.0 ± 11.7	< 0.1
Cu*	160	33.7	4.6	174 ± 31	2.8
Zn*	109	94.7	3.8	101 ± 6	1.1
As	< 2.4	0.80	0.15	< 1.7	0.10
Se	< 1.8	0.62	0.37	< 1.9	0.25
Br	< 0.3	< 0.2	0.12	< 0.2	0.11
Rb*	49.6	92.1	13.3	42.5 ± 18.8	1.1
Sr*	185	285	20.3	225 ± 20	2.0
Y*	96.9	77.8	10.4	43.2 ± 9.0	1.5
Zr*	155	563	29.4	203 ± 53	21
Nb*	9.3	47.6	0.7	15.0 ± 3.8	0.2
Sb	< 0.2	0.10	0.06	< 0.2	0.03
Cs	1.36	1.09	0.25	0.68 ± 0.30	0.12
Ba*	297	912	163	370 ± 89	4.7
La	30.4	68.5	6.08	25.4 ± 7.3	2.18
Ce	38.0	132	8.59	42.2 ± 13.0	4.10
Nd	28.7	64.0	6.57	25.4 ± 6.34	1.69
Sm	8.24	16.0	1.89	6.65 ± 1.38	0.40
Eu	2.53	3.99	0.54	1.90 ± 0.29	0.07
Gd	11.1	12.4	1.64	6.53 ± 1.55	0.33
Tb	1.64	2.00	0.29	1.04 ± 0.26	0.04
Tm	0.88	1.04	0.13	0.63 ± 0.12	0.03
Yb	6.12	5.82	0.79	3.68 ± 0.89	0.16
Lu	0.96	0.83	0.11	0.58 ± 0.14	0.03
Hf	4.15	13.1	0.80	4.99 ± 1.27	0.51
Ta	0.58	2.79	0.07	0.96 ± 0.20	0.03
Ir (ppb)	< 2.1	< 1.4	< 0.4	< 2.2	< 0.3
Au (ppb)	1.57	1.48	< 0.3	1.35 ± 0.46	0.04
Pb*	9.2	12.5	3.6	6.9 ± 1.1	1.4
Th	4.59	8.66	0.71	3.10 ± 0.79	0.57
U	< 0.6	2.44	0.19	0.57 ± 0.06	0.17
K/U	48,110	12,930	27,380	25,100 ± 12,400	1547
Zr/Hf	63.9	49.1	65.5	55.7 ± 3.3	33.6
La/Th	6.62	7.91	8.59	8.17 ± 0.24	3.83
Hf/Ta	7.17	4.68	12.2	5.15 ± 0.27	19.6

Table 1. *Continued*. Major and trace element contents in samples collected outside the studied structures of target rock equivalents compared to shocked lithologies from within the structure.

	Samples collected outside the structure			Shocked lithologies	
	Serra Geral basalt	Rhyodacite	Botucatu sandstone	Brecciated volcanic rocks (average $n = 3$)	Monomict sandstone breccia
Th/U	7.65	3.55	3.78	5.43 ± 1.02	3.30
La_N/Yb_N	3.36	7.95	5.22	4.63 ± 0.23	9.38
CIA	51	59	41	50 ± 1	59

All the elements marked with * in wt%, the remaining trace elements in ppm, except as noted. All the major elements and the minor elements marked with * were measured with XRF, the remnant trace elements were measured with INAA. All Fe as Fe_2O_3. N = chondrite-normalized (see Mader and Koeberl [2009] for further explanation). CIA (Chemical Index of Alteration) = $(Al_2O_3/[Al_2O_3 + CaO + Na_2O + K_2O]) \times 100$ in molecular proportions. All ratios are the average of the ratios calculated for each sample.

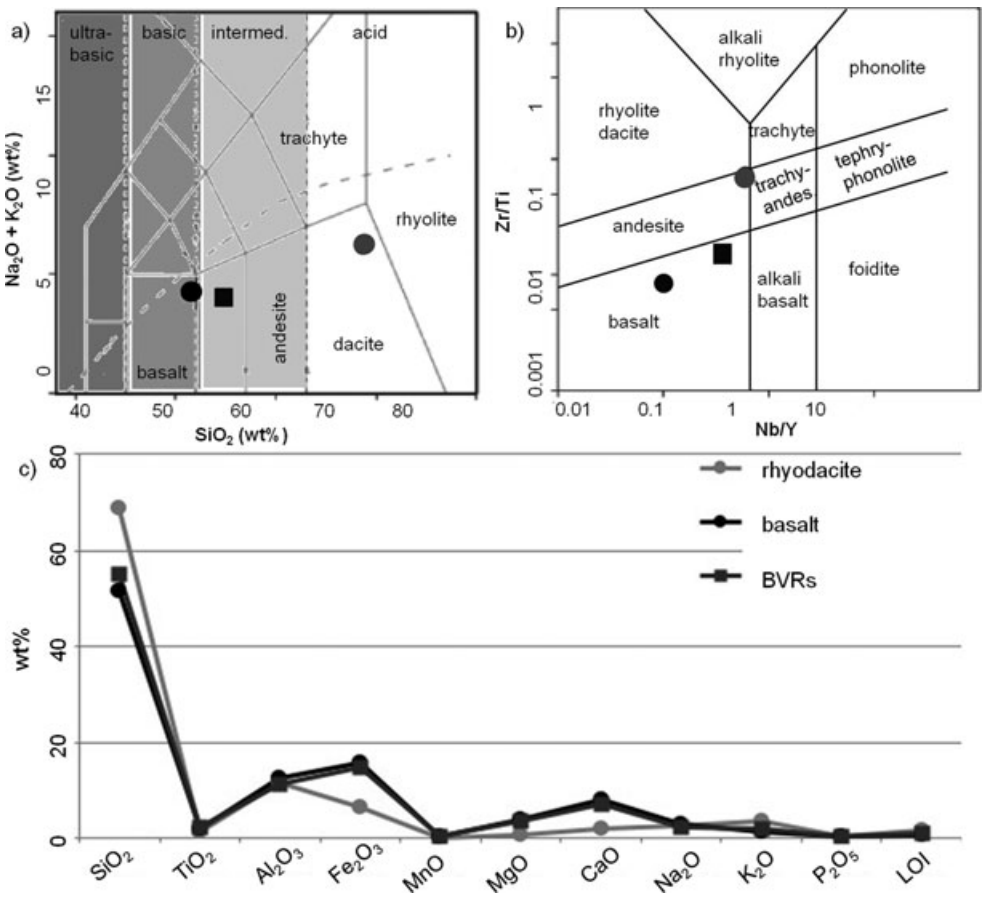

Fig. 10. Geochemical classification of the BVR compared with the target rocks, from data listed in Table 1. a, b) Geochemical classification for volcanic rocks after Le Bas et al. (1986) and Janousek et al. (2006). The Serra Geral basalt is shown as a black circle, the Serra Geral rhyodacite as a gray circle, the BVR (average of three analyses) as a black square. The BVRs fall between the basalt and the rhyodacite in composition, but closer to the basalt. c) Major element composition of the target lithologies listed in Table 1 (Serra Geral basalt and rhyodacite, Botucatu sandstone) and the BVR (average of three analyses).

forming the so-called "core-and-mantle" structure (for terminology, see Passchier and Trouw 1998). Very few quartz grains show shock features, as described below. The geochemical data of the sandstone breccia, compared to the Botucatu sandstone, are given in Table 1. The bulk composition yields a more pure sandstone than the Botucatu sandstone, showing enrichment in SiO_2 (+3.2% compared to the Botucatu sandstone) and strong decrease in Al_2O_3 (−74%), CaO (−94%), and K_2O (−88%). Even though no hematite was observed in the brecciated sandstone, the iron content is only a quarter less than that of the Botucatu sandstone.

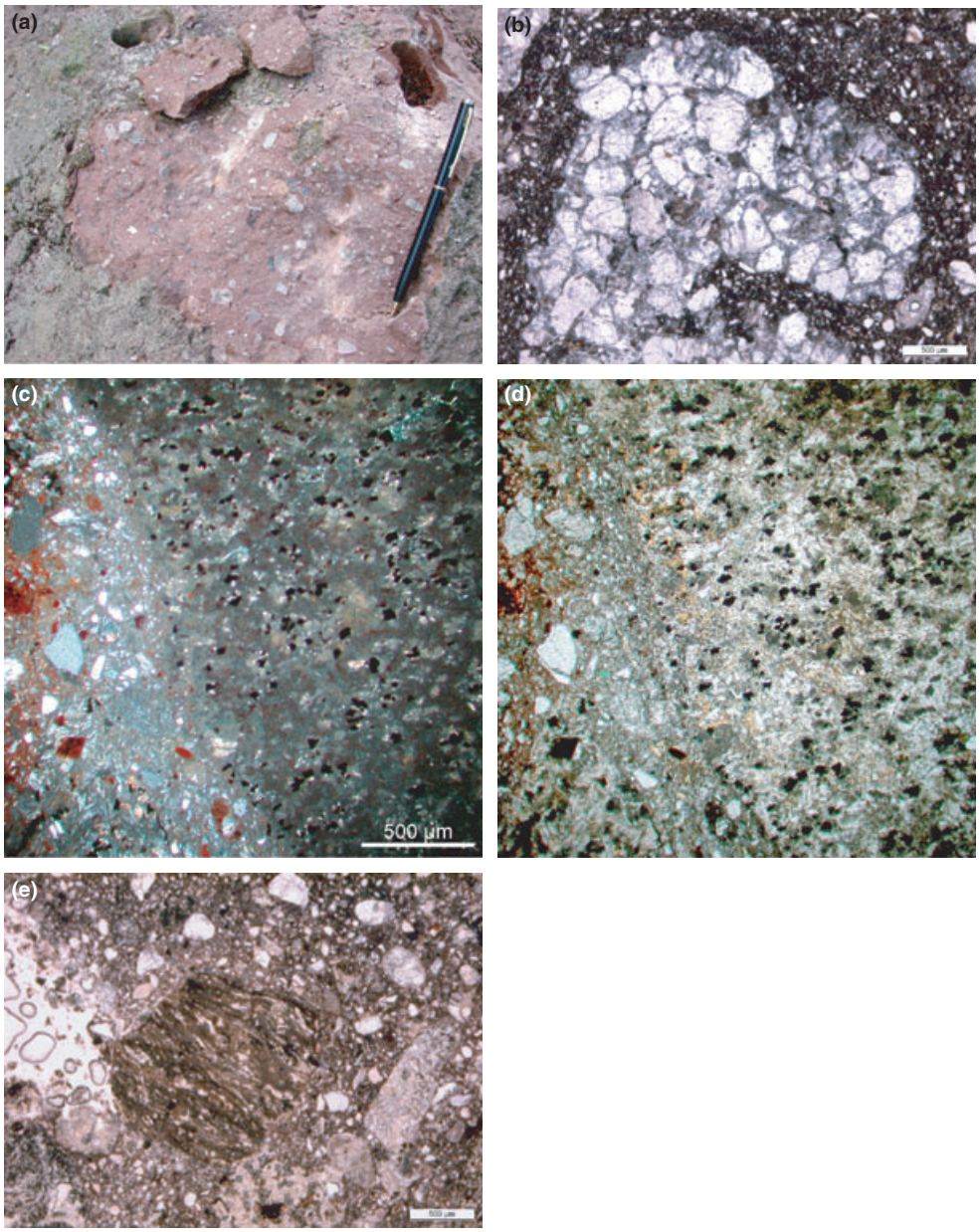

Fig. 11. Polymict breccia from near the center of the structure (S26°48.90′/W52°09.75′). a) Outcrop view of polymict breccia, showing basalt clasts as well as minor amounts of sandstone and calcite clasts in a fine-grained red matrix. b) Detail of a clast of sandstone in the polymict breccia, with fractured quartz. Plane-polarized light image. c) Clast of shocked basalt (on the right-hand side of the image) in the polymict breccia. The pyroxene is fractured and the plagioclase is partially transformed into diaplectic glass, as suggested by its isotropic extinction. Plane-polarized light. d) Same as in 11c in cross-polarized light. e) Detail of a melt clast, with internal fluidal texture. To the left of the clast, there is frothy silica melt. Plane-polarized light image.

SHOCK METAMORPHIC FEATURES

The occurrence of diagnostic shock metamorphic features at Vargeão Dome, such as planar fractures (PFs), planar deformation features (PDFs), and shatter cones, has been briefly reported by Hachiro et al. (1993), Kazzuo-Vieira et al. (2004), and Crósta et al. (2006). Here, we review these occurrences, and present some new evidence of shock metamorphism at Vargeão Dome.

Shatter cones in sandstones were reported by Crósta et al. (2006) from the Ghisolfi sand pit (Figs. 13a and 13b). They form individual cones of 12–25 cm in size.

However, we recently found shatter cones in basalt near the center of the structure, in a couple of outcrops

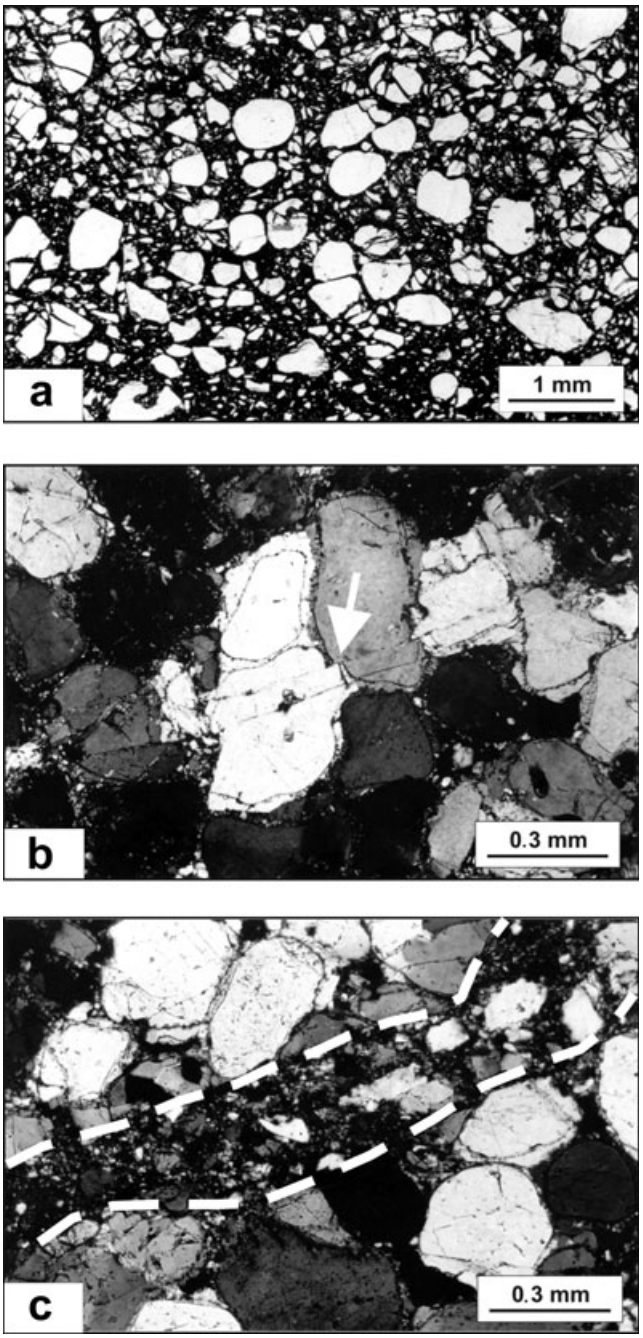

Fig. 12. Monomict sandstone breccia from the Ghisolfi sandstone pit. a) Undeformed sandstone clast in the monomict sandstone breccia, showing rounded quartz grains with pure silica and hematite cement. Cross-polarized light image. b) Monomict sandstone breccia with the original rounded quartz grains developing epitaxial growth of pure quartz. Cross-polarized light image. c) Shear zone in the breccia, marked by white dashed lines, containing fragmented quartz. Cross-polarized light image.

located a few hundred meters from that of the polymict breccias (see Fig. 6 for location). These shatter cones comprise aggregates of small nested cones, with individual cones ranging in size from 2 to 7 cm (Figs. 13c and 13d); they are similar (but smaller) to the ones found in the Vista Alegre impact crater (Crósta et al. 2010b). The shatter cones are formed in fine-grained basalt, which otherwise is apparently unshocked, and contains volcanic glass, with incipient crystallization and devitrification, and randomly distributed mm-sized euhedral hexagonal opaque minerals. A reddish layer appears decorating the striated surface, possibly constituting alteration or melt, but not resolvable under the optical microscope.

The alleged presence of PDFs (Hachiro et al. 1993) could not be confirmed in the samples analyzed herein. However, a pebble from one of the conglomeratic layers found at the Ghisolfi sand pit shows the presence of so-called feather features (Figs. 14a and 14b). This type of shock feature has been described by French et al. (2004) and was recently discovered in samples from many impact structures worldwide (Kenkmann and Poelchau 2009; Poelchau and Kenkmann 2011). Feather features occur as short, parallel to subparallel lamellae with a similar spacing as planar deformation features (PDF). These lamellae are always found in combination with a planar fracture (PF) from which they emanate. Feather features are crystallographically controlled and mainly occur along (0001), $10\bar{1}\bar{1}$, and $11\bar{2}\bar{2}$. The feather features observed herein are developed along (0001) planar fractures crosscutting the whole pebble and form angles of 50°–60° with respect to the main fracture (Figs. 14a and 14b). The majority of the observed feather feature lamellae emanate from the PF. Microscopic analysis of quartz grains with feather features shows that their formation is linked to shearing along the associated PF during shock deformation (Poelchau and Kenkmann 2011). The generation of shear fractures with feather features in plane wave shock recovery experiments suggests a pressure range of approximately 7–10 GPa, although further constraints are needed for an upper and lower pressure limit (Poelchau and Kenkmann 2011). In the recent formation model, feather features are believed to be formed by tensile stresses during rapid shock unloading. The release of strong lattice strain along the planar fracture (PF) causes the concentration of feather features at the planar fracture.

Another shock feature observed at Vargeão Dome is diaplectic glass after plagioclase in shocked basalt clasts of the polymict breccia (Figs. 11c and 11d).

SEISMIC ANALYSIS OF THE SUBSURFACE STRUCTURE OF VARGEÃO DOME

Despite the filtering procedure applied to the reflection seismic data, the resulting section has still a considerable amount of noise. This is a result of the limitations of the original data acquisition techniques

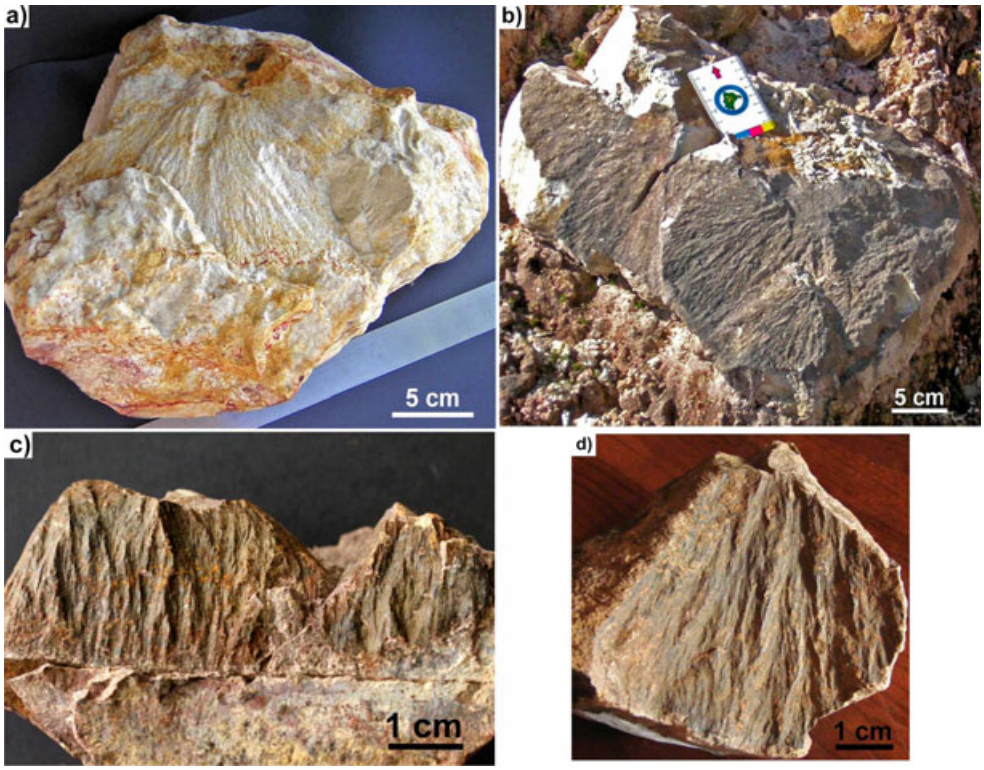

Fig. 13. Shatter cones from the Vargeão structure. a and b) Shatter cones in sandstone found in the Ghisolfi pit (S26°49.05′/W52°10.87′). c and d) Shatter cones in basalt (S26°48.90′/W52°09.75′).

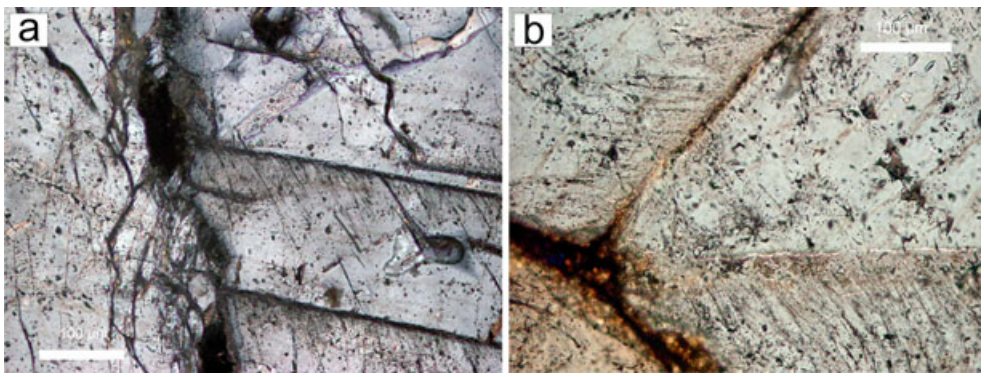

Fig. 14. Feather features (FF) in quartz emanating from (0001) planar fractures (PF) (a), and in addition from {10–11} (b). Some feather features in (b) are curvilinear at their tip suggesting that they propagate as cracks without crystallographic control. Figures (a) and (b) are from a pebble in the sandstone conglomerate (Botucatu/Pirambóia Formation) from the Ghisolfi sand pit (S26°49.05′/W52°10.87′). For more information, see text.

used in the early 1980s, combined with the fact that the thick sequence of basaltic rocks usually do not favor the acquisition of good quality seismic data. There is an upper seismic zone where the signal-to-noise ratio (SNR) is higher, thus allowing a more detailed interpretation of the geologic features, an intermediate zone with poor SNR, and a lower zone with good SNR. The boundary between the upper and intermediate zones can be placed at depths between 1000 and 2000 m outside the structure, as observed in the continuous depth point (CDP) seismic section across the structure that is shown in Fig. 15a.

The interpretation of the section (Fig. 15b) is focused mainly on structures (faults) and on zones of distinct seismic signatures, aiming to correlate them with the different stratigraphic units shown in the geologic profile of borehole RCH-0001-SC. The faults were interpreted based on the discontinuities of the amplitudes

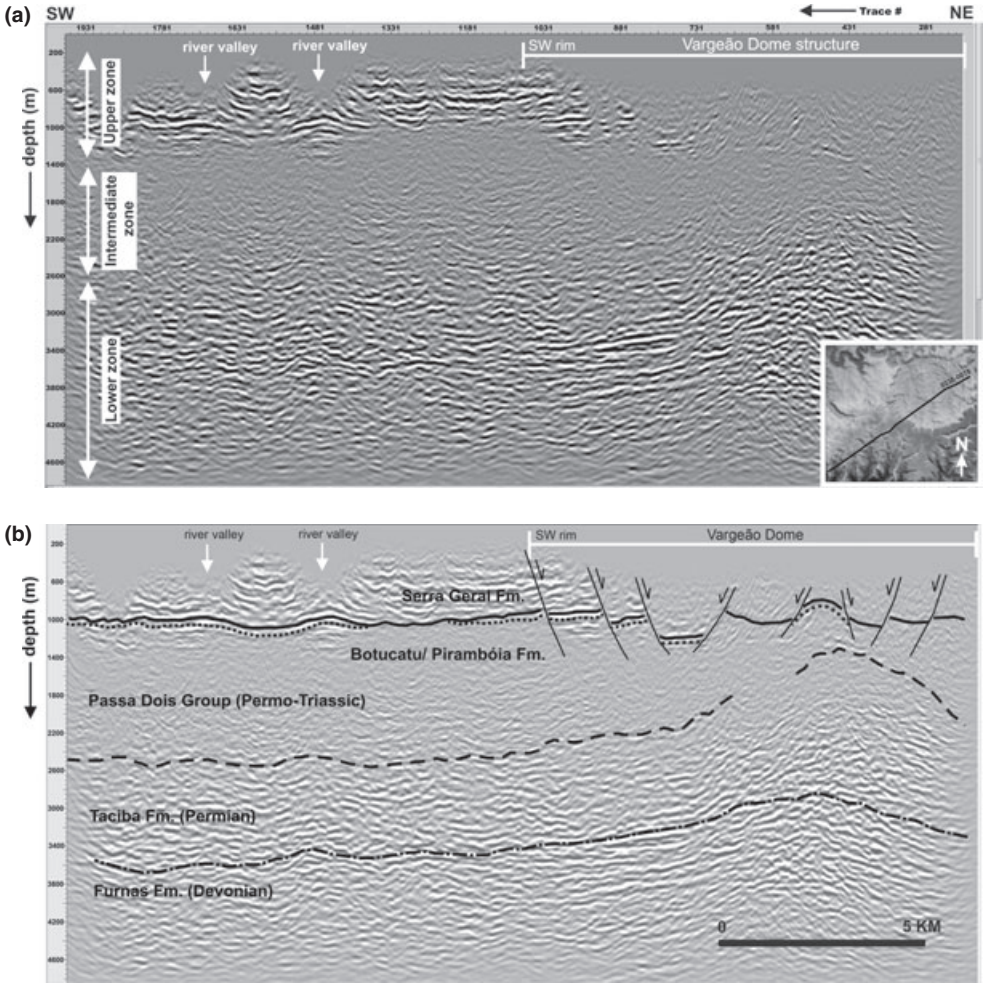

Fig. 15. a) Continuous depth point (CDP) seismic section across the Vargeão Dome; the inset shows the location of the section over the DEM; b) Interpretation of the stratigraphy underneath Vargeão Dome and its main structural features. See also Fig. 4 for location of the segment of the seismic section across Vargeão Dome.

of the seismic signal, and compared to lineaments interpreted from the remote sensing data.

A comparison of the topographic elevation profile along line 00236-0078, shown in the upper right part of Fig. 15, with the seismic section indicates that the rim of Vargeão coincides with subvertical discontinuities of the upper seismic zone, attributed to the upper lava flows comprising rhyodacite and tholeiitic basalt. This suggests the occurrence of listric faults along the rim of the structure, with a downward displacement of blocks from the upper layers of volcanic rocks of the Serra Geral Formation into the interior of the structure. These subvertical discontinuities of this upper reflector only occur at the rim and are not observed outside the structure.

The upper seismic zone is attributed to the volcanic sequences of the Serra Geral Fm., which in this portion of the Paraná Basin has a thickness of approximately 950 m, and the Botucatu/Pirambóia sandstones, with a thickness of approximately 100 m. The bottom of the Serra Geral Fm. is clearly seen in the upper seismic zone (solid line in Fig. 15b), at a depth of approximately 950 m outside Vargeão Dome, as well as the base of the Botucatu/Pirambóia sandstones, at a depth of approximately 1050 m (dotted line in Fig. 15b).

Moving from the rim toward the center of Vargeão Dome, on the right-hand half of Fig. 15b, the upper seismic zone is barely visible from the approximate position of the left rim, with the exception of some small and discontinuous portions located between the rim and the central area. Most of the interior of the structure is dominated by signatures typical of the intermediate seismic zone.

In the center of Vargeão, the intermediate zone, which corresponds to the Permian Passa Dois Group, is considerably thinned, by at least a factor of two. This

can be interpreted as a result of stratigraphic uplift of the Botucatu/Pirambóia Fm. and Passa Dois Group (Permo-Triassic). The Taciba Fm. (Permian) and Funas Fm. (Devonian) correspond to the lower seismic zone and they also appear to have been uplifted, although not as much as the upper units (Fig. 15b).

Using the depth information from well 1RCH-0001-SC, together with the differences in seismic signatures, the possible contact between the Passa Dois Gr. and the Taciba Fm. was interpreted at a depth of 2500 m outside Vargeão Dome (dashed line in Fig. 15b) and of 1300 m near the center of the structure (Fig. 15b). Likewise, the contact between the Taciba Fm. and the Furnas Fm., sitting at 3500 m outside the structure (dotted-dashed line in Fig. 15b), seems to be raised to a depth of 3000 m near its center.

The uplift of the stratigraphic units underneath Vargeão Dome produces a conical structure observed in the right-hand side of the section shown in Fig. 15, which roughly coincides with the center of the structure. Within this conical structure, a zone of high disturbance of the seismic signals can be observed, with little or no lateral continuity of the reflectors, which suggests strong deformation of the rocks.

Around the central uplift of the structure, which is clearly seen on the seismic section, slivers of Botucatu/Pirambóia sandstones were apparently brought to the surface. The likely mechanism for this can be a combination of the uplift of the underlying units, and the vertical faulting around the central uplift; erosion may have played a role in partially exposing these sandstones as well.

DISCUSSION

The concentric multiannular pattern observable in Vargeão Dome in remote sensing images and DEM, bounded by a sharp and steep rim around almost its entire circumference, stands out remarkably in the volcanic plateaus of the Serra Geral Formation. The interior of the structure is a circular depression with a rim diameter of approximately 12.4 km. Concentric and radial lineaments are present in the interior of the structure, as well as in a slightly elevated central portion. These morphologic characteristics comply with those pointed out by French (1998) and French and Koeberl (2010) for complex impact craters.

The presence of a central uplift at Vargeão Dome is also implied by the surficial occurrence of sandstones attributed to the Botucatú/Pirambóia formations, which normally lie at a depth of approximately 1000 m in this part of the Paraná Basin, according to the stratigraphic column obtained from nearby oil exploration well 1RCH-0001-SC (ANP 1981). Uplifting of the lower sedimentary units that lay underneath the center of the Vargeão Dome, in particular, the ones immediately below the Serra Geral Formation, i.e., the Botucatu/Pirambóia sandstone and the sequences belonging to the Passa Dois Group, is also evident in the seismic section across the structure (see Fig. 15). The structural uplift of approximately 1 km for Vargeão Dome is consistent with the data presented by Cintala and Grieve (1998) for terrestrial craters with a diameter of 12.4 km.

A central uplift diameter of about 3 km is estimated based on the circumference of the faulted and exposed sandstone blocks, assuming that its external boundary represents the extent of the central uplift.

The structural characteristics of Vargeão Dome are summarized in Fig. 15b, based on the interpretation of seismic and remote sensing data, and supported by field observations. There seem to be a number of listric faults associated with Vargeão Dome, from the rim to the central portion. The faults at the rim coincide with the topographic gradient that marks almost the entire circumference of the crater, and are responsible for the tilting of the blocks of the upper volcanic unit, producing the large blocks of rhyodacite that occur at the interior of the structure. The faults in the zone located between the rim and the center are the likely source of the internal multiannular structure depicted in the remote sensing images. Finally, the subvertical faults associated with the central uplift were responsible for vertical movements that brought the stratigraphic units underlying the Serra Geral Formation (e.g., the Botucatú/Pirambóia sandstones) to the surface. At this stage, it is not yet clear how the sandstones formed a collar of faulted blocks, surrounding the central uplift.

The rocks that occur at the interior of the Vargeão structure exhibit very peculiar deformation features of different types and intensities, which are not seen in equivalent rocks outside the structure. Deformation and brecciation are commonly observed in all rock samples from the interior of the structure, except for a collar approximately 1.5–2 km wide near the rim, in which the rocks (mostly basalts) are only affected by faulting (Fig. 7). The listric faults in this zone are mostly subvertical and dip inwards, and we interpret them as the result of the collapse that led to the formation of the external rim of the structure. These faults were responsible also for moving large blocks of rhyodacite from the upper lava flows in this region, and also of basalt from the intermediate ones, toward the interior of the structure. These large blocks are currently found in this peripheral zone, with little or no deformation.

Within this collar, and extending toward the center of the structure, the volcanic rocks exhibit different levels of deformation, usually characterized by brecciation. The spatial distribution of the deformed volcanic rocks showing different intensities of brecciation (BVR) cannot

be established at the current level of mapping, but appears to be irregular. The inner zone of Vargeão Dome, where BVR are present, is not circular but ellipsoidal, with the long axis in the NW/SE direction (Fig. 6). BVR appear to be quite different from the polymict breccia, with a wider variety of lithologies observed in the latter. Nevertheless, the presence of sandstone fragments in the reddish veins does not allow classifying them as monomict basalt breccias.

The chemical data show that the BVR have a composition largely similar to that of the unshocked basalt, with slight SiO_2 enrichments. As the enrichment in SiO_2 is not accompanied by enrichment in Al_2O_3 and alkalis, a minor contribution from the sandstone, rather than from an acid volcanic member, is indicated, and is confirmed by the general petrographic observations. The same trend is displayed by the trace elements (Table 1). The chemical index of alteration (CIA; [Table 1]; Nesbitt and Young 1982) represents the alteration state of the rock and is given by the ratio between Al_2O_3 wt% and the sum of Al_2O_3 wt%, Na_2O wt%, K_2O wt%, and CaO wt%*. CaO wt%* means the total measured amount of CaO wt% minus the fraction contained in calcite and apatite. The XRF method does not allow the measurement of the carbon content, and so the amount of calcite was not estimated. Petrographic observations indicate that only negligible amounts of calcite are present. The apatite contribution was estimated from the content of F, measured by XRF. The resulting CIA values in the BVR are similar to those of unshocked basalt (Table 1), confirming the petrographic observations that these rocks are barely altered (Nesbitt and Young 1982). In general, there is no enrichment in the abundance of alkalis, and the freshness of plagioclase and pyroxene in the BVR, and the similarity of the trace elements contents to those in the target basalts exclude the presence of extensive postimpact hydrothermal alteration. Further studies of the BVR are in progress to help understand their formation.

The geochemical analysis of the monomict sandstone breccia reveals that it is composed almost exclusively of SiO_2, and the petrographic study confirms that it is more sorted than the Botucatu/Pirambóia sandstone. In contrast to the Botucatu sandstone, the monomict sandstone breccia contains mostly quartz, and no feldspar, mica, or hematite was observed. Not surprisingly, the monomict sandstone breccia thus contains lower amounts of Al_2O_3, CaO, and K_2O compared to the Botucatu/Pirambóia sandstone (Table 1). Due to the limited variation in composition, the few samples analyzed are considered representative. The petrographic study showed that the quartz grains are almost devoid of shock features, such as PF, PDF, and feather features. Together with the observed brittle comminution along shear zones, characterized by limited incipient recrystallization, this suggests that the monomict sandstone breccia has been formed through a brittle tectonic process, probably related to the uplift and subsequent collapse of the central part of the structure. The brittle deformation, which has produced pervasive fracturing of the monomict sandstone breccia, probably has favored fluid circulation, which might explain also the disappearance of feldspars by solution.

Among the lithologies collected within the crater, the chemical analyses presented herein are limited to the BVR and the monomict sandstone breccia. Both rocks show no significant enrichments in elements, such as Co, Ni, or Cr; in addition, the amount of Ir is below the detection limit (less than 2 ppb for both the lithologies) of the methods employed herein. Furthermore, the Cr content, compared to the detection limit for Ir, is consistent with the expected content in the continental crust (see review in Koeberl 2007) for both the unshocked basalt and the BVR. Thus, at this time, there is no evidence for the presence of a meteoritic component in the rocks within the crater, despite the occurrence of melt clasts that are probably locally produced and not volcanic. More detailed analyses on the various lithologies, including the polymict breccia, are planned to better constrain these preliminary observations.

Although fragments of shocked basalt characterized by the complete isotropization of plagioclase were found in the polymict breccia, we cannot apply the shock stage classification compiled by Kieffer et al. (1976) because the shocked material has been reworked in the polymict breccia and cannot be replaced to its pristine (preimpact) position/depth. On the other hand, the monomict sandstone breccia contains tectonic deformation features, such as conjugate sets of shear zones and not shock deformation, such as low shock pressure features like planar fractures and feather features in quartz. We relate the lack of the latter to the current degree of erosion of the structure, which likely caused the partial exhumation of the Botucatu/Piramboia sandstones. These strata, being originally at approximately 1 km under the volcanic rocks, were less affected by the shock. The uncommon appearance of basalt "fragments" in the BVR, with rounded smooth margins, fresh plagioclase, and preserved residual pockets of glass, is subject to further investigation to understand their formation in relation to the magmatic flows, the impact, and the postimpact alteration.

CONCLUSIONS

Although having been proposed as an impact structure for more than two decades, very little information on Vargeão Dome has been available in the literature. Here, we present, for the first time, a summary of the geology

and impact features of this structure, which has an apparent diameter of 12.4 km and was formed in volcanic rocks of the Serra Geral Formation within the Paraná Basin in southern Brazil.

The lava flows in which the crater was excavated comprise an upper layer of rhyodacite (Chapecó Unit) and several layers of basalt (Alto Uruguai Unit). The thickness of the volcanic package in this region is estimated at 1000 m. The excavation affected also the underlying sedimentary units, exposing sandstone in the central portion of the structure. These sandstones have, therefore, been uplifted by approximately 1100–1200 m.

The structure exhibits the morphologic characteristics of a complex impact crater, as shown by optical and microwave remote sensing data for surficial features, and also by seismic data for subsurface structures. These characteristics include a sharp and steep rim formed by listric faults dipping inwards, concentric and radial fractures in the interior of the structure resulting in a multiannular pattern, and subvertical faults dipping mostly outwards in the collar of the central uplift. The diameter of the central uplift is approximately 3 km and it is marked by the occurrence of a collar of sandstone of the Botucatu/Pirambóia formations.

The rocks that occur at the interior of Vargeão Dome are mainly brecciated volcanics (mainly basalt, with subordinate amounts of rhyodacite) and monomict sandstone breccias. Polymict breccias were found at two nearby locations, bearing mainly clasts of basalt and sandstone in a red matrix of basalt, rhyodacite, quartz, and calcite. Geochemically, these rocks are largely similar in composition to the unshocked equivalent lithologies from outside the structure. No contribution from meteoritic material has been identified so far.

Shock features identified in Vargeão Dome comprise shatter cones, feather features, and diaplectic feldspar glass. The shatter cones developed in basalt and in sandstone from the interior of the central uplift. This is the second occurrence of shatter cones in basalt known on Earth, the other being at the Vista Alegre structure, also formed in Serra Geral basalt (Crósta et al. 2010b). Feather features were found in a pebble from a conglomeratic layer of the Botucatu/Pirambóia formations and have developed along (0001) planar fractures. According to Poelchau and Kenkmann (2011), feather features are a type of shock feature developed in quartz subject to shock pressure approximately 7–10 GPa; therefore, in the lower portion of the shock metamorphism regime. Diaplectic glass was found in basalt clasts in the polymict breccia.

Acknowledgments—This project received funding from the Barringer Family Fund for Meteorite Impact Research, Fundação de Amparo à Pesquisa no Estado de São Paulo (FAPESP) (grants 01/01068-0 and 04/03295-2), Conselho Nacional de Desenvolvimento Científico e Tecnológico (CNPq) (grants 305203/2003-7 and 303065/2004-4), Fundo de Apoio ao Ensino, Pesquisa e Extensão (FAEPEX) of the University of Campinas (UNICAMP) (grant 475/2003), and the Austrian Science Foundation FWF (grant P21821-N10, to CK). Antonio Rizzi, from Petrobras, is acknowledged for his support in seismic data processing. Dieter Mader and Peter Nagl from the University of Vienna are thanked for sample preparation and for help with the chemical analyses. We appreciate the constructive reviews by E. Buchner, J. Ormö, and J. Plescia, as well as editorial comments and suggestions by W. U. Reimold.

Editorial Handling—Dr. Uwe Reimold

REFERENCES

Abrams M. 2000. The Advanced Spaceborne Thermal Emission and Reflection Radiometer (ASTER)—Data products for the high spatial resolution imager on NASA's EOS-AM1 platform. *International Journal of Remote Sensing* 21:847–861.

ANP (Agência Nacional de Petróleo). 1981. *Perfil composto do poço 1RCH 0001 SC (Rio Chapecó)*. Unpublished internal document. Rio de Janeiro, Brazil: National Petroleum Agency (ANP).

Barbour Jr. E. and Corrêa W. A. G. 1981. *Geologia da estrutura de Vargeão, SC*. Unpublished Technical Report. Brazil: PAULIPETRO—Consórcio CESP/IPT. 33 p.

Brown R. J., Brisco B., D'Iorio M., Prévost C., Ryerson R. A., and Singhroy V. 1996. RADARSAT applications: Review of GlobeSAR Program. *Canadian Journal of Remote Sensing* 22:404–419.

Cintala M. J. and Grieve R. A. F. 1998. Scaling impact melting and crater dimensions: Implications for the lunar cratering record. *Meteoritics & Planetary Science* 33:889–912.

Crósta A. P. 1982. *Estruturas de impacto no Brasil: Uma síntese do conhecimento atual*. Proceedings, 32° Congresso Brasileiro de Geologia, Salvador, Brazil: Sociedade Brasileira de Geologia. pp. 1372–1377.

Crósta A. P. 1987. Impact structures in Brazil. In *Research in terrestrial impact structures*, edited by Pohl J. Braunschweig-Wiesbaden: Friedrich Vieweg & Sohn. pp. 30–38.

Crósta A. P. 2004. Impact craters in Brazil: How far we've gotten (abstract). *Meteoritics & Planetary Science* 39:A27.

Crósta A. P., Kazzuo-Vieira C., Choudhuri A., and Schrank A. 2006. Vargeão Dome Astrobleme, State of Santa Catarina: A meteoritic impact record on volcanic rocks of the Paraná Basin. In *Sítios Geológicos e Paleontológicos do Brasil vol. 2*, edited by Winge M., Schobbenhaus C., Berbert-Born M., Queiroz E. T., and Campos D. A. Brasília, DF: SIGEP/DNPM. pp. 1–12.

Crósta A. P., Lourenço F. S., and Priebe G. H. 2010a. Cerro do Jarau, Rio Grande do Sul: A possible new impact structure in southern Brazil. In *Large meteorite impacts and planetary evolution IV*, edited by Gibson R. L. and Reimold W. U. GSA Special Paper 465. Boulder, Colorado: Geological Society of America. pp. 173–190.

Crósta A. P., Koeberl C., Furuie R., and Kazzuo-Vieira C. 2010b. The first description and confirmation of the Vista Alegre impact structure in the Paraná flood basalts of southern Brazil. *Meteoritics & Planetary Science* 45:181–194.

Feldman V. I., Sazonova L. V., Mironov Y., Kapustkina I. G., and Ivanov B. A. 1983. Circular structure Longancha as possible meteorite crater in basalts of the Tunguska syneclise (abstract). 14th Lunar and Planetary Science Conference. pp. 191–192.

Fredriksson K., Dube A., Milton D. J., and Balasundaram M. S. 1973. Lonar Lake, India: An impact crater in basalt. *Science* 180:862–864.

Freitas M. A., Caye B. R., and Machado J. L. F. 2002. *Projeto Oeste de Santa Catarina (PROESC): Diagnóstico dos recursos hídricos subterrâneos do oeste do Estado de Santa Catarina*. Unpublished Technical Report. 110 p. Brasilia: CPRM/ Governo do Estado de Santa Catarina.

French B. M. 1998. *Traces of catastrophe: A handbook of shock-metamorphic effects in terrestrial meteorite impact structures*. Houston: Lunar and Planetary Institute. 130 p.

French B. M. and Koeberl C. 2010. The convincing identification of terrestrial meteorite impact structures: What works, what doesn't, and why. *Earth-Science Reviews* 98:123–170.

French B. M., Cordua W. S., and Plescia J. B. 2004. The Rock Elm meteorite impact structure, Wisconsin: Geology and shock-metamorphic effects in quartz. *Geological Society of America Bulletin* 116:200–218.

Fudali R. F., Milton D. J., Fredriksson K., and Dube A 1980. Morphology of Lonar crater, India: Comparison and implications. *Moon and Planets* 23:493–515.

Hachiro J., Coutinho J. M. V., Frascá M. H. B. de O., and Menezes C. M. 1993. *O astroblema de Vargeão (SC): Evidências petrográficas de um crateramento criptoexplosivo por petardo extraterrestre*. 3° Simpósio de Geologia do Sudeste Rio de Janeiro, Brazil: Sociedade Brasileira de Geologia. pp. 276–281.

Janousek V., Farrow C. M., and Erban V. 2006. Interpretation of whole-rock geochemical data in igneous geochemistry: Introducing Geochemical Toolkit (GCDkit). *Journal of Petrology* 47:1255–1259.

Kazzuo-Vieira C. 2009. *Caracterização geológica e geofísica da estrutura de impacto Domo de Vargeão, SC*. MSc thesis, University of Campinas, Campinas, SP, Brazil. 142 p.

Kazzuo-Vieira C., Crósta A. P., and Choudhuri A. 2004. Impact features from Vargeão Dome, Southern Brazil. (abstract). *Meteoritics & Planetary Science* 39:A52.

Kazzuo-Vieira C., Crósta A. P., Gamboa F., and Tygel M. 2009. Caracterização geofísica da estrutura de impacto do Domo de Vargeão, Brasil. *Revista Brasileira de Geofísica* 27:375–388.

Kenkmann T. and Poelchau M. H. 2009. Low-angle collision with Earth: The elliptical impact crater Matt Wilson, Northern Territory, Australia. *Geology* 37:459–462.

Kieffer S. W., Schaal R. B., Gibbons R., Hörz F., Milton D. J., and Dube A. 1976. Shocked basalt from Lonar Impact Crater, India, and experimental analogues. Proceedings, 7th Lunar Science Conference. pp. 1391–1412. Pergamon Press, New York.

Koeberl C. 1993. Chicxulub crater, Yucatán: Tektites, impact glasses, and the geochemistry of target rocks and breccias. *Geology* 21:211–214.

Koeberl C. 2007. The geochemistry and cosmochemistry of impacts. In *Treatise on geochemistry*, online edition, vol. 1, edited by Davis A. Oxford: Elsevier. pp. 1.28.1–1.28.52, doi: 10.1016/B978-008043751-4/00228-5.

Le Bas J., Le Maitre R. W., Streckeisen A., and Zanettin B. 1986. A chemical classification of volcanic rocks based on the total alkali-silica diagram. *Journal of Petrology* 27:745–750.

Mader D. and Koeberl C. 2009. Using instrumental neutron activation analysis for geochemical analyses of terrestrial impact structures: Current analytical procedures at the University of Vienna geochemistry activation analysis laboratory. *Applied Radiation and Isotopes* 67:2100–2103.

Maloof A. C., Stewart S. T., Weiss B. P., Soule S. A., Swanson-Hysell N. L., Louzada K. L., Garrick-Bethell I., and Poussart P. M. 2010. Geology of Lonar crater, India. *Geological Society of America Bulletin* 122:109–126.

Mantovani M. S. M., Stewart K., Turner S., and Hawkesworth C. J. 1995. Duration of Paraná magmatism and implications for the evolution and source regions of continental flood basalts. *Anais da Academia Brasileira de Ciências* 67:163–169.

Milani E. J. 2004. Comentários sobre a origem e evolução tectônica da Bacia do Paraná. In *Geologia do Continente Sul-americano: Evolução da Obra de Fernando Flávio de Almeida*, edited by Mantesso-Neto V., Bartorelli A., Carneiro C. D. R., and Brito-Neves B. B. de. São Paulo: Ed. Beca, pp. 265–280.

Mironov Y. V., Ladygin V. M., Pchelintseva N. F., Kuz'min N. R., and Ryakhovskiy V. M. 1987. Low pressure impact breccias from basalts of Logancha astroblem (abstract) (in Russian). All-Union Meteorite Conference, Tallinn, pp. 30–32.

Nesbitt H. and Young G. M. 1982. Early Proterozoic climates and plate motions inferred from major element chemistry of lutites. *Nature* 299:715–717.

Osae S., Misra S., Koeberl C., Sengupta D., and Ghosh S. 2005. Target rocks, impact glasses, and melt rocks from the Lonar impact crater, India: Petrography and geochemistry. *Meteoritics & Planetary Science* 40:1473–1492.

Paiva Filho A., Andrade C. A. V. de., and Scheibe L. F. 1978. *Uma janela estratigráfica no oeste de Santa Catarina: O Domo de Vargeão*. 30° Congresso Brasileiro de Geologia, Recife, Brazil: Sociedade Brasileira de Geologia. pp. 408–412.

Passchier C. W. and Trouw R. A. J., 1998. *Microtectonics*. Berlin: Springer Verlag. 366 p.

Peate D. W. 1997. The Paraná-Etendeka Province. In *Large igneous provinces: Continental, oceanic, and planetary flood volcanism*, edited by Mahoney J. and Coffin M. Washington, DC: American Geophysical Union Geophysical Monograph. pp. 217–245.

Peate D. W. and Hawkesworth C. J. 1996. Lithospheric to asthenospheric transition in Low-Ti flood basalts from southern Parana, Brazil. *Chemical Geology* 127:1–24.

Peate D. W., Hawkesworth C. J., and Mantovani M. S. M. 1992. Chemical stratigraphy of the Parana lavas (South America): Classification of magma types and their spatial distribution. *Bulletin of Volcanology* 55:119–139.

Poelchau M. H. and Kenkmann T. 2011. Feather features: A low shock pressure indicator in quartz. *Journal of Geophysical Research* 116, B02201, 13 p., doi:10.1029/2010JB007803.

Rabus B., Eineder M., Roth A., and Bamler R. 2003. The Shuttle radar topography mission: A new class of digital elevation models acquired by spaceborne radar. *ISPRS Journal of Photogrammetry and Remote Sensing* 57:241–262.

Renne P., Ernesto M., Pacca I. G., Coe R. S., Glen J. M., Prévot M., and Perrin M. 1992. The age of Paraná flood volcanism, rifting of Gondwanaland, and the Jurassic-Cretaceous boundary. *Science* 258:975–979.

Sengupta D. and Bhandari N. 1988. Formation age of Lonar crater (abstract). 19th Lunar and Planetary Science Conference. pp. 1059–1060.

Son T. H. and Koeberl C. 2007. Chemical variation in Lonar impact glasses and impactites. *GFF* 129:161–176.

Stewart K., Turner S., Kelly S., Hawkesworth C., Kirstein L., and Mantovani M. 1996. 3-D, ^{40}Ar—^{39}Ar geochronology of the Paraná continental flood basalt province. *Earth and Planetary Science Letters* 143:95–109.

Turner S., Regelous M., Kelley S., Hawkesworth K., and Mantovani M. S. M. 1994. Magmatism and continental break-up in the South Atlantic: High precision ^{40}Ar-^{39}Ar geochronology. *Earth and Planetary Science Letters* 121:333–348.

Yilmaz O. 2001. Fundamentals of signal processing. In *Seismic data processing*. *Investigations in geophysics* vol. 1, 2nd ed., edited by Neitzel E. B. and Doherty S. M. Tulsa, OK: Society of Exploration Geophysicists. pp. 25–127.